Author(s): Jaakkola, Salla; Penttinen, Reetta; Vilen, Silja; Jalasvuori, Matti; Rönnholm, Gunilla; Bamford, Jaana; Bamford, Dennis; Oksanen, Hanna

Title: Closely Related Archaeal Haloarcula hispanica Icosahedral Viruses HHIV-2 and SH1 Have Nonhomologous Genes Encoding Host Recognition Functions

Year: 2012

Version:

Please cite the original version:

Jaakkola, S., Penttinen, R., Vilen, S., Jalasvuori, M., Rönnholm, G., Bamford, J., Bamford, D., & Oksanen, H. (2012). Closely Related Archaeal Haloarcula hispanica Icosahedral Viruses HHIV-2 and SH1 Have Nonhomologous Genes Encoding Host Recognition Functions. Journal of Virology, 86(9), 4734-4742. https://doi.org/10.1128/JVI.06666-11

JVI Journals.ASM.org

Closely Related Archaeal *Haloarcula hispanica* Icosahedral Viruses HHIV-2 and SH1 Have Nonhomologous Genes Encoding Host Recognition Functions

Salla T. Jaakkola,[a] Reetta K. Penttinen,[b] Silja T. Vilén,[a]* Matti Jalasvuori,[b] Gunilla Rönnholm,[c] Jaana K. H. Bamford,[b] Dennis H. Bamford,[a] and Hanna M. Oksanen[a]

Institute of Biotechnology and Department of Biosciences, University of Helsinki, Helsinki, Finland[a]; Department of Biological and Environmental Science and Nanoscience Center, Jyväskylä, Finland[b]; and Institute of Biotechnology, University of Helsinki, Helsinki, Finland[c]

Studies on viral capsid architectures and coat protein folds have revealed the evolutionary lineages of viruses branching to all three domains of life. A widespread group of icosahedral tailless viruses, the PRD1-adenovirus lineage, was the first to be established. A double β-barrel fold for a single major capsid protein is characteristic of these viruses. Similar viruses carrying genes coding for two major capsid proteins with a more complex structure, such as *Thermus* phage P23-77 and haloarchaeal virus SH1, have been isolated. Here, we studied the host range, life cycle, biochemical composition, and genomic sequence of a new isolate, *Haloarcula hispanica* icosahedral virus 2 (HHIV-2), which resembles SH1 despite being isolated from a different location. Comparative analysis of these viruses revealed that their overall architectures are very similar except that the genes for the receptor recognition vertex complexes are unrelated even though these viruses infect the same hosts.

Viruses with a common virion architecture that infect hosts from different domains of life have been shown to share a similar coat protein fold despite the lack of detectable sequence similarity (1, 3, 34). Viruses have been grouped into structure-based lineages in which the major capsid protein (MCP) folds and, occasionally, similar genome packaging machineries serve as indicators for common ancestry. One such structural lineage, the PRD1-adenovirus lineage, consists of icosahedral viruses with double-stranded DNA (dsDNA) genomes (1, 3, 10, 11, 16, 34). Recent findings suggest that this lineage divides into two subgroups (24, 25, 26, 27). The subgroups consist of viruses with similar overall capsid architectures, homologous packaging ATPases, and, with the exception of adenovirus, internal membranes underneath the icosahedral capsids. One of these subgroups is well established, and it includes several viruses for which high-resolution MCP structures have been determined, e.g., PRD1 (16), adenovirus (49), *Paramecium bursaria* chlorella virus 1 (PBCV-1) (38), PM2 (2), *Sulfolobus* turreted icosahedral virus (STIV) (46), and vaccinia virus (8). In all cases, the monomeric MCP harbors two distinct β-barrels formed by eight β-sheets, also referred to as double β-barrel MCP. The viruses belonging to the other less-studied subgroup have two MCPs instead of one. For this subgroup, no high-resolution structures of the MCPs are yet available. *Haloarcula hispanica* virus SH1 (14, 24, 29, 43), *Thermus thermophilus* phage P23-77 (25, 26), *Thermus aquaticus* phage ϕIN93 (37), *Salisaeta* icosahedral phage 1 ([SSIP-1] A. P. Aalto, D. Bitto, J. J. Ravantti, D. H. Bamford, J. T. Huiskonen, and H. M. Oksanen, submitted for publication), *Haloarcula* plasmid pHH205 (58), and several proviruses (26, 27) belong to this subgroup.

The estimated astronomical number of virus particles in the biosphere ($>10^{31}$) creates a massive selective pressure on cellular organisms (10, 17, 53, 55). It has also been realized that viruses are a crucial factor in the global ecosystem and are likely to harbor the greatest genetic diversity on Earth (53, 55). Hypersaline environments such as salt lakes and salterns with near-saturation NaCl content are able to support the growth of rich microbial cell populations that consist mainly of euryarchaeal cells belonging to the family *Halobacteriaceae* (41). The number of virus-like particles in hypersaline environments is also high, and viruses are the only predators in such environments (22, 52). Today, close to 60 haloarchaeal viruses have been characterized, presenting head-tailed (myo-, sipho-, and podovirus), spindle-shaped, icosahedral, and pleomorphic virus morphotypes (7, 42). However, recent observations of virus-like particles in hypersaline environments proposed a wider diversity of virus morphologies (52). Haloviruses have been found to infect host cells from different locations around the world that have similar environmental conditions. This has led us to consider the hypersaline environments as a single habitat bridged by microbial networks (7).

Only one tailless icosahedral haloarchaeal virus, SH1, has been characterized (43, 48). SH1 is a virulent virus infecting euryarchaeal *H. hispanica* (43). It has a linear dsDNA genome of 30,898 bp with 309-bp inverted terminal repeats (ITRs), 5′-terminal proteins, and 56 predicted open reading frames (ORFs) (14, 44). The virion is composed of at least 15 different structural proteins (VP1 to VP15, where VP is virion protein), which have been divided into three categories: vertex, capsid, and membrane associated (24, 29). Its horn-like spikes with 2-fold symmetry are composed of proteins VP3 and VP6, which are most probably involved in receptor recognition. The vertex structure also contains the glycine-serine-rich protein VP2 with heptapeptide repeats character-

Received 25 November 2011 **Accepted** 13 February 2012
Published ahead of print 22 February 2012
Address correspondence to Hanna M. Oksanen, hanna.oksanen@helsinki.fi.
* Present address: Haartman Institute, Department of Virology, University of Helsinki, Helsinki, Finland.
S.T.J. and R.K.P. contributed equally to this article.
Supplemental material for this article may be found at http://jvi.asm.org/.

doi:10.1128/JVI.06666-11

istic of coiled-coil proteins. The protein-rich membrane of SH1 consists of cardiolipin, phosphatidylglycerol, phosphatidylglycerophosphate methyl ester, and phosphatidylglycerosulfate, which are selectively incorporated from the host membrane into the virion during virus assembly (14). The selective incorporation of lipids into the virus membrane has also been described for other viruses with an internal membrane (36). The capsid, arranged in a T=28 lattice, is composed of two MCPs: VP4 (25.7 kDa) and VP7 (20.0 kDa) (24). The capsomers are decorated with either two or three towers (24).

Here, we report the characterization of *H. hispanica* icosahedral virus 2 (HHIV-2), a second icosahedral tailless halophilic dsDNA virus containing an inner membrane. We also compared the properties of HHIV-2 with those of SH1. The two viruses have significant similarities at the genomic and protein levels, as well as unique properties. Thus, this study provides insight into the evolution of archaeal viruses.

MATERIALS AND METHODS

Viruses, cells, media, and growth conditions. The archaeal strains and viruses used in this study were *H. hispanica* ATCC 33960 (28), *Haloarcula* sp. PV7 (7), SH1 (named according to its isolation location, serpentine lake and host "hispanica" [43]), and HHIV-2 (7). Cells were grown aerobically at 34/37°C in modified growth medium (MGM) (19, 40). Artificial 30% (wt/vol) salt water (SW) contained 240 g of NaCl, 30 g of $MgCl_2 \cdot 6H_2O$, 35 g $MgSO_4 \cdot 7H_2O$, 7 g of KCl, 5 ml 1 M $CaCl_2 \cdot 2H_2O$, and 80 ml of 1 M Tris-HCl (pH 7.2) per liter. The salt water was used as the base of MGM and diluted to concentrations of 18% (top-layer agar), 20% (plates), and 23% (liquid). In addition, MGM contained 5 g of peptone (Oxoid, Hampshire, England) and 1 g of Bacto yeast extract (Becton, Dickinson and Company, Sparks, MD [BD]) per liter. Bacto agar (BD) was used to prepare plates (14 g/liter) or top-layer agar (4 g/liter). For thin-section electron microscopy, we used modified MGM in which Tris-HCl (pH 7.2) was replaced with 4-morpholine ethanesulfonic acid (pH 7.2).

Growth and purification of viruses. Virus stocks were prepared by mixing top-layer agar from confluent plates with 2 ml of broth per plate. After 1.5 h of shaking (37°C), lysates were cleared by centrifugation (10,823 × *g* for 20 min at 4°C; Sorvall SLA3000 rotor). For large-scale liquid growth of HHIV-2, an early-logarithmic phase culture of *H. hispanica* (6.0×10^8 CFU/ml) was infected with HHIV-2 virus stock using a multiplicity of infection (MOI) of 5 to 20. Cultures were incubated overnight at 34°C with aeration. After lysis, cell debris was removed by low-speed centrifugation (10,823 × *g* for 30 min at 4°C; Sorvall SLA3000 rotor). Virus particles were precipitated from the cleared lysate with 10% (wt/vol) polyethylene glycol 6000 with magnetic stirring (at 4°C for 1 h), collected by centrifugation (10,823 × *g* for 1 h at 4°C; Sorvall SLA3000 rotor), and resuspended in HHIV-2 buffer (20 mM Tris-HCl [pH 7.2], 20 mM $MgCl_2$, 10 mM $CaCl_2$, and 0.5 M NaCl). The virus was purified in a linear 5 to 20% (wt/vol) sucrose (HHIV-2 buffer) gradient (83,641 × *g* for 40 min at 20°C; Sorvall AH629 rotor), and the light-scattering virus zone was collected. This product was designated "once-purified" virus. The particles were collected by centrifugation (113,580 × *g* for 3 h at 20°C; Sorvall T647.5 rotor) and resuspended in HHIV-2 buffer. When appropriate, the once-purified virus was layered on top of CsCl solution ($\rho = 1.4$ g/ml in HHIV-2 buffer) and centrifuged to equilibrium (83,641 × *g* at 16 h for 20°C; Sorvall AH629 rotor). The particles purified in CsCl were diluted in HHIV-2 buffer in a volume ratio of 1:1 (virus to solution) and collected by centrifugation as described above. The concentrated CsCl purified material was designated "twice-purified" virus. For virion density analyses, the CsCl gradient was fractionated into 1-ml fractions. The infectivity, A_{260}, and density of each fraction were measured, and the fractions were analyzed by sodium dodecyl sulfate (SDS)-polyacrylamide gel electrophoresis (PAGE). SH1 was grown on *H. hispanica* and purified as previously described (29, 43). Purified HHIV-2 virions were negatively stained with 3% (wt/vol) ammonium molybdate (pH 7.6). The micrographs were taken with a JEOL 1200EX transmission electron microscope operating at 80 kV (Electron Microscopy Unit, Institute of Biotechnology, University of Helsinki).

Life cycle of HHIV-2 and thin-section electron microscopy of HHIV-2-infected cells. To optimize the virus production in liquid culture, cell densities ranging from 6.0×10^8 to 9.5×10^8 CFU/ml (optical density at 550 nm [OD_{550}] of 0.7 to 0.9) and MOIs ranging from 5 to 40 were tested. For one-step growth experiments, a mid-logarithmic-phase culture of *H. hispanica* (9.0×10^8 CFU/ml; at 37°C) was infected with HHIV-2 virus stock using an MOI of 10. At 1 h postinfection (p.i.), the cells were collected (10,823 × *g* at 30 min for 22°C; Sorvall SLA3000 rotor) and resuspended in fresh medium to remove unbound viruses. A noninfected culture was used as a control and treated in the same manner. Concomitantly with turbidity measurements (OD_{550}), free viruses were assayed by taking samples at 1-h intervals. The cells were removed by centrifugation (16,060 × *g* for 10 min; Biofuge Pico), and the number of free viruses in the supernatant fraction was determined by a plaque assay.

The number of released progeny viruses was calculated from a single-step experiment in which an MOI of 7 was used to infect the cells (6.7×10^8 CFU/ml) at 37°C. Unbound viruses were removed by centrifugation (10,823 × *g* for 30 min at 22°C; Sorvall SLA3000 rotor) at 1 h p.i., and the amount of progeny viruses was determined by a plaque assay.

For thin-section electron microscopy of noninfected and HHIV-2-infected cultures of *H. hispanica*, cultivation was performed as described above, except that the MOI was 80 and the infected cell density was 6.0×10^8 CFU/ml. Unbound viruses were removed at 30 min p.i. as described above. Thin-section electron microscopy was performed as previously described (13). Micrographs were taken with a JEOL 1200EX electron microscope operating at 80 kV (Electron Microscopy Unit, Institute of Biotechnology, University of Helsinki).

Adsorption assays. An early-logarithmic-phase culture of *H. hispanica* or *Haloarcula* sp. PV7 was infected with HHIV-2 or SH1 (MOI of 2.7×10^{-4}) and incubated at 22 or 37°C without aeration for 2 h. Samples were taken at 20-min intervals, and adsorption was stopped by diluting the cells 1:100 in ice-cold broth. The cells were removed (16,060 × *g* for 10 min; Biofuge Pico), and the reduction in the number of PFU in the supernatant was determined by a plaque assay using *H. hispanica* as a host. The rate of adsorption was calculated with the formula $k = 2.3 \times \log(P_0/P)/B_t$, where B represents the concentration of host cells, P_0 represents the concentration of free viruses at time point zero, and P represents the concentration of free viruses at the end of the experiment after a period of time t (4).

HHIV-2 stability. The thermal stability of HHIV-2 was examined by incubating samples of HHIV-2 lysate in 23% MGM for 30 min at different temperatures (0, 22, 30, 40, 50, 60, and 70°C), followed by a plaque assay. HHIV-2 stability in solutions of depleted ionic strength was examined by diluting HHIV-2 lysates (1:100) in modified HHIV-2 buffers containing 0, 100, 200, 300, or 400 mM NaCl or in modified HHIV-2 buffers with no Ca^{2+} or Mg^{2+}. The samples were incubated at 4°C for 2 h and for 24 h for buffers with no Ca^{2+} or Mg^{2+}. Virion stability was determined by a plaque assay.

Protein analyses. The protein concentration of purified virus was measured by the Coomassie blue method (18) using bovine serum albumin as a standard. The protein composition of the virion was analyzed using an 8, 14, or 17% polyacrylamide-tricine-SDS gel (51). SDS-PAGE gels were stained with either Coomassie brilliant blue or Sudan Black B (Sigma-Aldrich). The structural proteins were identified by either N-terminal sequencing or mass spectrometric analyses of the tryptic peptides (partial amino acid sequences of the peptides) in the Protein Chemistry Core Laboratory, Institute of Biotechnology, University of Helsinki, as described previously (14).

Genome sequencing and sequence analyses. The genome was extracted from twice-purified virus particles diluted 1:10 in water using SDS

and proteinase K (final concentrations of 2% and 100 μg/ml, respectively). To extract DNA without protease treatment, only SDS was added (final concentration of 0.5%). After incubation (at 37°C for 1 h) nucleic acids were extracted with phenol and ether and precipitated with sodium chloride and ethanol. The purified genome was treated with DNase I (final concentration of 0.5 mg/ml; Sigma-Aldrich) or digested with a selection of 23 different restriction enzymes.

Isolated DNA was digested with SalI, SmaI, HincII, or Eco321. DNA fragments were ligated into pSU18 or pSU19 (15) cloning vectors digested with either SalI or SmaI. The clones were sequenced, and the obtained sequences were used to design oligonucleotides for primer walking using genomic DNA as a template. The sequencing was performed using the Sanger sequencing method with an automatic sequencer (Applied Biosystems 3130*xl* Genetic Analyzer) and a BigDye Terminator, version 3.1, Cycle Sequencing Kit (Applied Biosystems). Base calling and sequence refining were performed with Sequencing Analysis, version 5.2.0 (Applied Biosystems). Both DNA strands were sequenced at least twice, giving 4-fold coverage for each base pair (except region 6284 to 6410, where the other strand was sequenced only once). Regions at the ends of the genome (approximately 400 bp) were sequenced in one direction toward the genome end using several specific primers. The ORFs were determined, and similar sequences were searched using BLAST (5), after which the resulting nucleotide and amino acid sequences of the corresponding ORFs were aligned. To execute the computational genomic stages described above, Vector NTI, version 11.0 (Invitrogen), was used. The possible presence of transmembrane helices in HHIV-2 amino acid sequences was predicted with TMHMM, version 2.0 (http://www.cbs.dtu.dk/services/TMHMM/) (33).

Nucleotide sequence accession number. The HHIV-2 genome was submitted to the GenBank database under accession number JN968479.

RESULTS

HHIV-2 is a virulent virus. HHIV-2 infecting *H. hispanica* (Alicante, Spain) (28) was isolated from a saltern in Margherita di Savoia, Italy, while searching for new viruses in hypersaline environments (7). The screening of the host range of HHIV-2 using close to 80 different archaeal strains revealed that, in addition to its original isolation host, *Haloarcula* sp. PV7 from Trapani, Italy, was also susceptible to HHIV-2 (7). The plating efficiency of HHIV-2 on *H. hispanica* and *Haloarcula* sp. PV7 was the same (7), which was also the case with SH1 (data not shown).

In the single-cycle growth experiment of HHIV-2 using an MOI of 10, the host culture turbidity started to decrease at 4 to 5 h p.i. concomitantly with the increase in the number of free progeny viruses (Fig. 1A). Electron micrographs of thin-sectioned *H. hispanica* cells infected with HHIV-2 revealed a few virus-sized particles bound to the cell surface at 30 min p.i. (Fig. 1B) and a few putative empty procapsids and newly assembled viral particles inside the cells at 5 h p.i. (Fig. 1C and D). As a consequence of the cell lysis, the culture turbidity dropped an average of 0.23 optical density units (from the highest to the lowest point, 0.10 to 0.35; $n = 6$). The lysate titer was typically around 4.5×10^{10} PFU/ml (9.1×10^{9} to 9.0×10^{10} PFU/ml; $n = 6$). Based on single-cycle growth data, approximately 180 virus particles per infected cell were released ($n = 3$). We optimized the virus production using different cell growth phases and MOIs upon infection (see Materials and Methods). However, none of the conditions tested had any significant effect on the virus yield.

Adsorption assays of SH1 and HHIV-2 were conducted at 22°C and 37°C with *H. hispanica* and *Haloarcula* sp. PV7. The host or temperature used had no effect on the rate of adsorption with either of the viruses (data not shown). Adsorption of HHIV-2 and SH1 on *H. hispanica* at 22°C is shown in Fig. 1E. The adsorption

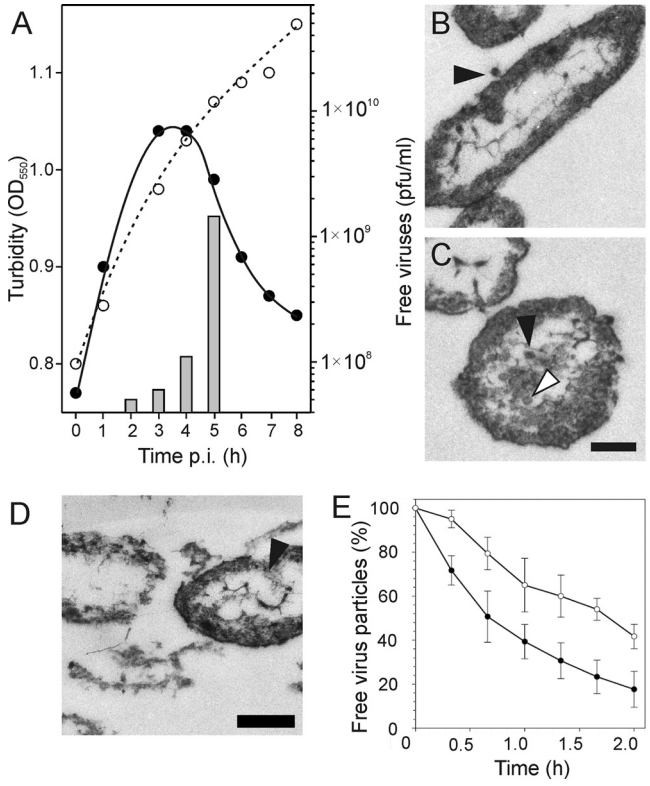

FIG 1 HHIV-2 life cycle. (A) One-step growth curve of HHIV-2 on *H. hispanica*. The cells were grown at 37°C and infected at an MOI of 10 at time point zero. Sixty minutes after infection, the cells were collected and resuspended in fresh medium to remove the nonadsorbed particles. The turbidity of uninfected (open circles) and infected (closed circles) cultures and the number of free viruses (gray bars) are shown. (B, C, and D) Thin section of HHIV-2 infected *H. hispanica* cells using an MOI of 80 at 0.5 (B) and 5 (C and D) h p.i. Black arrowheads point to virus particles. A white arrowhead points to a virus-sized empty particle. Scale bar, 200 nm. (E) Adsorption of HHIV-2 (closed circles) and SH1 (open circles) to *H. hispanica* at 22°C ($n = 3$).

rate constants calculated during the first hour p.i. for HHIV-2 and SH1 were 3.7×10^{-12} and 1.1×10^{-11} ml/min, respectively, showing that HHIV-2 binds slightly faster than SH1.

HHIV-2 is a membrane-containing complex virus. Surprisingly, the virus particle remained infectious under buffer conditions with low concentrations of NaCl (see Fig. S1A in the supplemental material). NaCl concentrations as low as 100 mM NaCl had no measurable effect on the virus titer after 24 h of storage. However, the total removal of NaCl reduced the titer by 2 orders of magnitude. There was a minimal effect on virus infectivity when magnesium and calcium were omitted from the buffer (see Fig. S1B). It seems that divalent cations are not absolutely necessary for virion stability. The virus was also stable at high temperatures up to 50°C (see Fig. S1C).

Virus particles obtained from liquid lysates were concentrated by polyethylene glycol precipitation and purified by rate zonal centrifugation in sucrose, resulting in a single infectious virus-containing zone. When the purified viruses from the sucrose gradient zone were subjected to equilibrium centrifugation in CsCl, a sharp infectious virus zone at the density of 1.33 g/ml was obtained (Fig. 2A). The recovery of infectious viruses during the purification process is shown in Table S1 in the supplemental material. Analysis of the CsCl-equil-

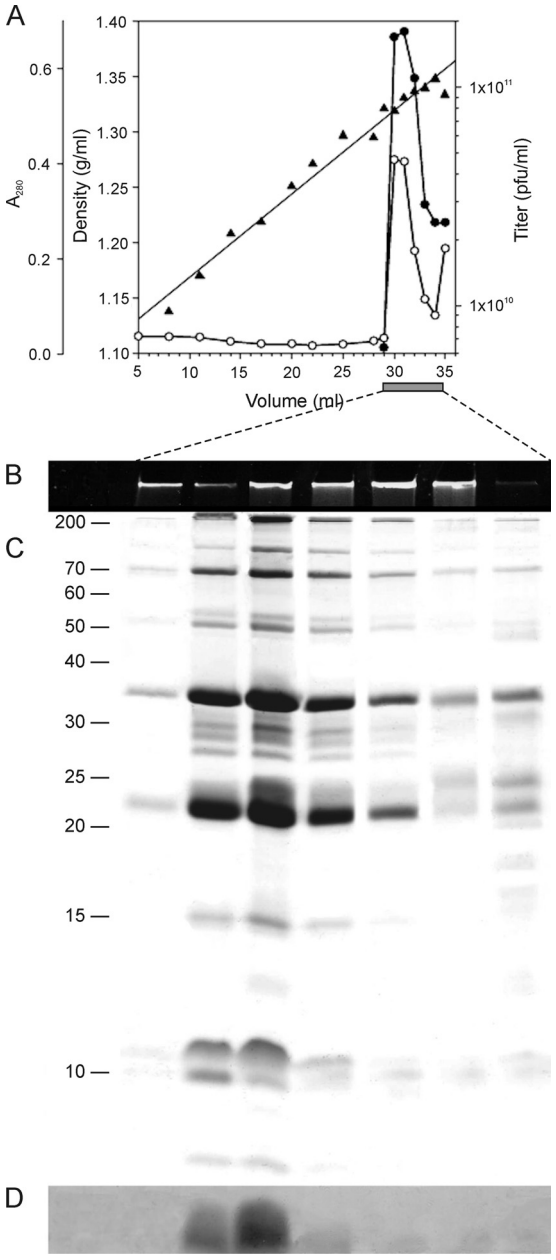

FIG 2 HHIV-2 virion composition. (A) Purification profile of HHIV-2 virion in a CsCl density gradient. The density (triangles), infectivity (closed circles), and A_{280} (open circles) of the gradient fractions are shown. (B) Nucleic acids in the upper SDS-PAGE gel stained with ethidium bromide. (C) Proteins separated in an SDS-PAGE gel stained with Coomassie blue. The molecular masses (kDa) of standard proteins are shown on the left. (D) Lipids in the SDS-PAGE gel are stained with Sudan Black B.

ibrated virus fractions by SDS-PAGE followed by staining of the stacking gel with ethidium bromide (for nucleic acid) and staining of the separation gel with Coomassie brilliant blue and Sudan Black B (for proteins and lipids, respectively) (Fig. 2B to D) revealed that the highly purified HHIV-2 virions were composed of nucleic acids, protein, and lipids. SDS-PAGE and Coomassie brilliant blue staining resolved 16 different protein species, which were directed to identification. The chloroform sensitivity (7) and low buoyant density of the particles (Fig. 2A) further suggested that HHIV-2 has a membrane component.

The protein pattern of HHIV-2 virion resembles that of the icosahedral halophilic virus SH1. The SDS-PAGE analysis of purified HHIV-2 and SH1 virions revealed that their protein profiles are rather similar but not identical (Fig. 3A). Both virions had two major protein species with similar apparent molecular masses (HHIV-2 VP4 and VP7, 25.9 and 19.8 kDa, respectively; SH1 VP4 and VP7, 25.7 and 20.0 kDa, respectively). Several other protein species in both viruses also migrated to similar positions.

The HHIV-2 virion proteins were identified using highly purified particles (Fig. 3A). Thirteen protein bands with molecular masses under 60 kDa were subjected to N-terminal sequence analysis. As a result, we obtained seven unique N-terminal sequences, all of which correlated with the translated gene products (VP4, VP5, VP7, VP10, VP12, VP16, and VP17) derived from the HHIV-2 genome sequence (Fig. 3B). In all of the determined N-terminal protein sequences, the first methionine had been removed. No host proteins or other impurities were detected. Four protein bands were subjected to identification by lipid chromatography with tandem mass spectrometry, which gave peptides belonging to HHIV-2 proteins VP1, VP2, VP18, and VP17 (Fig. 3; see also Table S2 in the supplemental material). In addition, there were four minor proteins associated with highly purified virions (VP13, VP14, VP19, and VP20). They did not yield any detectable signals in N-terminal sequencing.

The HHIV-2 proteins were named according to their relatedness to SH1 proteins. The HHIV-2 gene products resembling SH1 proteins VP1, VP2, VP4, VP7, VP10, VP12, and VP13 were named accordingly. HHIV-2 protein VP14 was identified on the basis of the similar mobility and seemingly similar copy number as SH1 VP14 in the SDS-PAGE gel (Fig. 3A). We detected two HHIV-2 virion-associated proteins, VP16 and VP17, with no match in SH1. A corresponding protein to HHIV-2 VP18 has not been detected in SH1, but SH1 ORF 55 shares significant similarity with HHIV-2 gene 42, which encodes VP18 (see Table S3 in the supplemental material). To summarize, the HHIV-2 virion contains at least 14 protein species with molecular masses ranging from approximately 4 to 200 kDa. Transmission electron microscopy visualized the HHIV-2 virions as tailless particles with a diameter of approximately 80 nm (Fig. 3C) (7). Based on the similarities with SH1 (see also below), we proposed a model for HHIV-2 virion organization (Fig. 3D).

HHIV-2 genome. The purified genome of HHIV-2 was cleavable with DNase I and digested with SmaI, XmaI, NotI, SalI, Eco321, and HincII. This demonstrates that the genome is a dsDNA molecule. Determination of the complete HHIV-2 genomic sequence revealed that the genome is a linear molecule of 30,578 bp with an overall GC content of 66.5% (Fig. 4A), which is typical not only for halophilic archaea (6, 9, 39) but also for haloviruses (14, 30, 47). The genome contains complementary identical 305-bp ITRs (Fig. 4A). Isolation of DNA from viruses, e.g., PRD1, Bam35, and SH1, without protease treatment leaves covalently linked terminal proteins attached to the linear dsDNA (12, 44, 45). Consequently, the DNA does not properly enter agarose gels. The HHIV-2 DNA isolated without protease treatment behaved in a similar manner, indicating that HHIV-2 most probably has covalently linked terminal proteins attached to the ends of its genome (see Fig. S2 in the supplemental material).

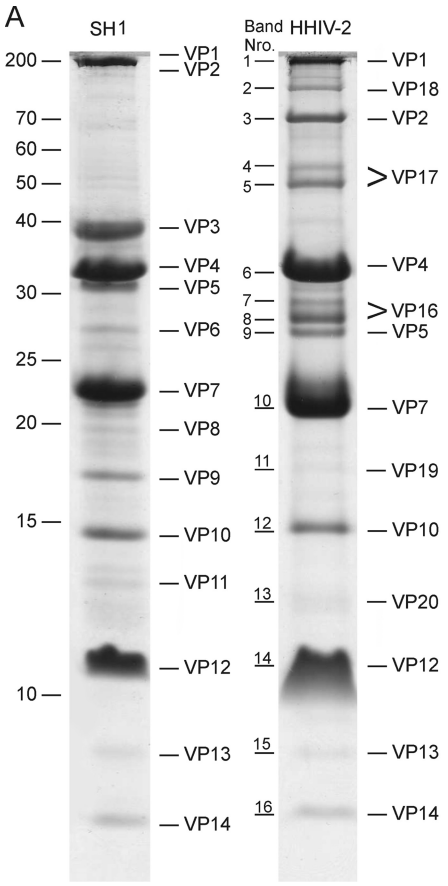

B

Band in the gel	N-terminal sequence[a]	Mass spectrometry[b]	HHIV-2 protein
1	nd	4	VP1
2	nd	4	VP18
3	nd	2	VP2
4	no sequence	5	VP17
5	GLSQATA	nd	VP17
6	ASQTQEYTIN	nd	VP4
7	ADLNDLD	nd	VP16
8	ADLNDLDTDS	nd	VP16
9	TIAAPF	nd	VP5
10	PEIGNGG	nd	VP7
11	no sequence	nd	VP19
12	GRLSAA	nd	VP10
13	no sequence	nd	VP20
14	ASINVNRATS	nd	VP12
15	no sequence	nd	VP13
16	no sequence	nd	VP14

[a] nd, not determined
[b] Number of identified specific peptides (sequences Table S2.)

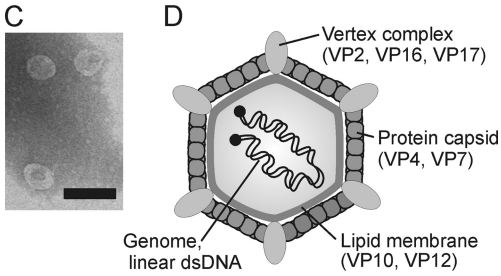

FIG 3 HHIV-2 virion and its structural proteins. (A) Protein composition of highly purified SH1 and HHIV-2 virions analyzed in a polyacrylamide-tricine-SDS gel (17% acrylamide) stained with Coomassie blue. The positions of SH1 and HHIV-2 structural proteins (VPs) are indicated. The sizes of the protein molecular mass standards (kDa) are shown on the left. The HHIV-2 protein bands (numbers 1 to 16) were directed to identification. (B) Identification of HHIV-2 virion structural proteins. (C) Transmission electron micrograph of highly purified HHIV-2 virions stained with 3% (wt/vol) ammonium molybdate (pH 7.6). Scale bar, 100 nm. (D) Model for HHIV-2 virion architecture.

The potential ORFs were assigned using a threshold of 72 bp as a minimum for the protein-encoding region. The HHIV-2 genome contains 43 putative ORFs, which are tightly packed in the genome. The properties of the ORFs and the encoded polypeptides are shown in Table S3 in the supplemental material. We also screened for putative ribosomal binding sites (RBSs) by comparing the sequences upstream from the start codon with the 3′-end of the host 16S rRNA gene sequence (AGGAG GTGA) (see Table S3). For most of the ORFs, a reasonable RBS was found. The distance between the RBS and start codon varied from 1 to 20 bp, with the average being 7 bp. According to the reading direction of the ORF clusters, the genes are organized in at least four operons (Fig. 4A). Ten ORFs were designated to encode the structural proteins of the virus (Fig. 3B; see also Tables S2 and S3) and thus were confirmed to be functional genes. Most of the genes encoding structural proteins are located in the middle of the genome and are most probably transcribed from a single operon (Fig. 4A). HHIV-2 genes 5 and 42, encoding structural proteins VP1 and VP18, respectively, are located separately from the other structural protein-encoding genes. HHIV-2 VP12 (gene 14) and four other hypothetical proteins (ORFs 2, 6, 12, and 27) have predicted transmembrane helices (Table S3).

Comparison of HHIV-2 and SH1 genome sequences suggests that the viruses have different components for host recognition. A BLAST search demonstrated that the genome of the halophilic archaea *Haladaptatus paucihalophilus* strain DX253 (RefSeq identifier NZ_AEMG01000000) contains an HHIV-2-related genome-integrated provirus, in which HHIV-2 ORFs/genes 4, 7 (putative ATPase), 9, 11, 13, 14 (VP12), 15 (MCP VP7), 16 (MCP VP4), 19 (VP2), 20 (VP5), and 21 (VP10) had homologous genes. The identities between the two HHIV-2 MCPs and the corresponding homologous proteins of *H. paucihalophilus* provirus were 48.5% and 48.4%, respectively. However, if we exclude SH1 and provirus hits, the BLAST search demonstrated that HHIV-2 genes encode proteins that have no clear homologues in current databases. Only HHIV-2 ORF 7 encodes a protein that is similar to other ATPase sequences. The putative HHIV-2 ATPase includes the classical Walker A and Walker B ATPase motifs (21, 57) along with the P9/A32-specific motif, which can be found in the putative packaging proteins of internal membrane-containing viruses, e.g., PRD1 and poxvirus (32, 54).

Both genome organization and gene and protein homologies showed that HHIV-2 and SH1 are closely related (Fig. 4A and B). The overall nucleotide similarity of these two genomes is 59.1%. The 309-bp-long ITR of SH1 was aligned with that of HHIV-2, showing 59.5% similarity, which corresponds to the overall ge-

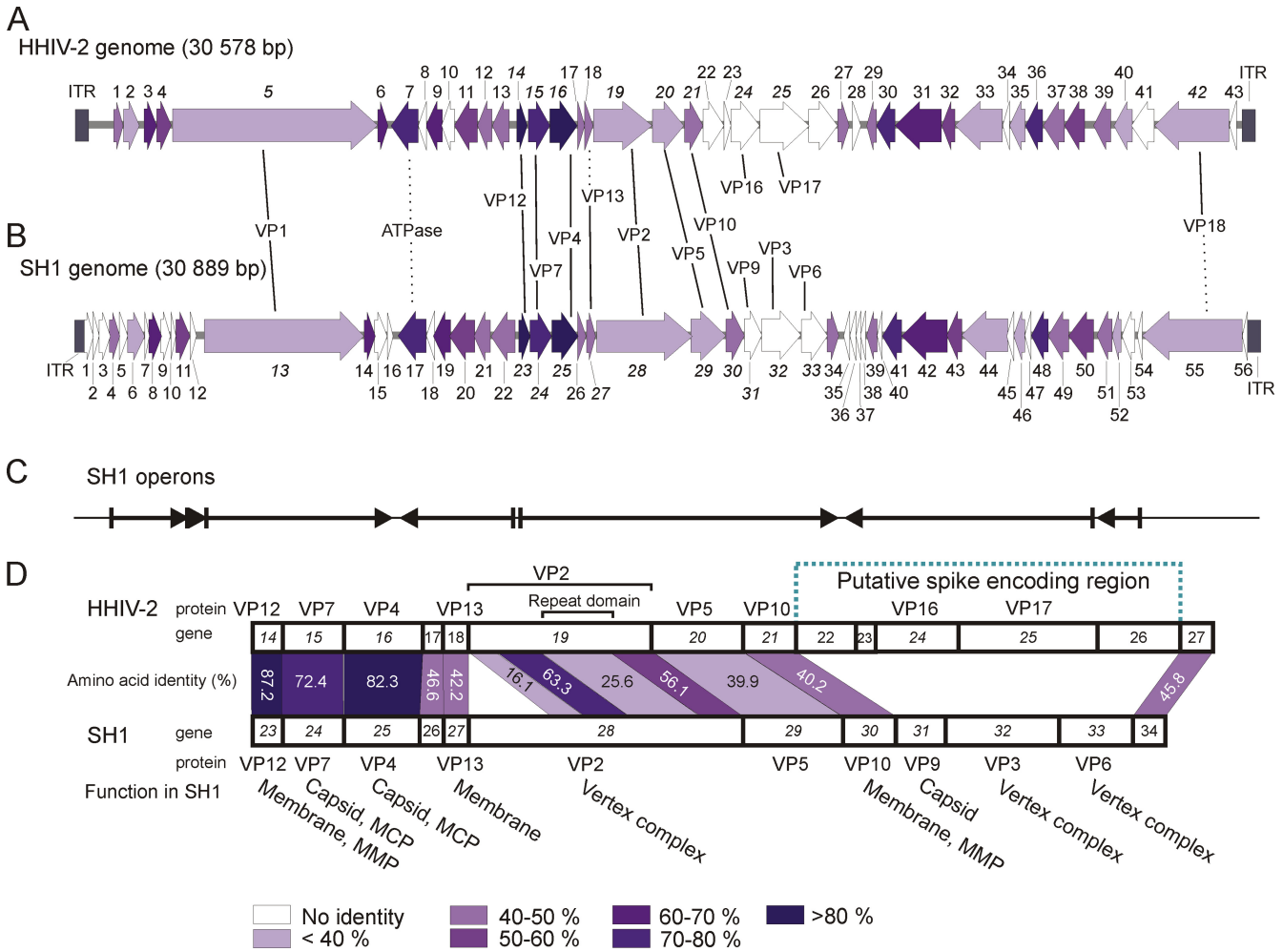

FIG 4 Comparison of the genome and protein sequences of HHIV-2 and SH1. (A and B) Numbers refer to ORFs and genes, and the arrows display their lengths and reading directions. Arrows are colored, as indicated on the figure, on the basis of the amino acid identity between the corresponding translated ORFs and genes of HHIV-2 (GenBank accession number JN968479) and SH1 (GenBank accession number AY950802). ITRs are marked with gray boxes. Solid lines refer to genes confirmed to be functional, and dashed lines refer to ORFs with corresponding genes confirmed to be functional in related virus species. (C) SH1 operons (44). (D) Alignment of the major structural protein coding regions of HHIV-2 and SH1. The amino acid identities (%) are given in between the related polypeptides. Identities for VP2 domains are calculated separately. The known functions of the SH1 proteins are indicated (MMP, major membrane protein; MCP, major capsid protein). The putative spike-encoding genomic region of HHIV-2 is bordered with a dashed line.

nome similarity. Additionally, the HHIV-2 and SH1 genes are organized in an analogous fashion, and their transcription directions are similar, allowing the assumption that HHIV-2 genes are also grouped in more than four operons, as concluded for SH1 (Fig. 4C) (44). Thirty-two of 43 putative HHIV-2 ORFs were related to SH1 ORFs. We used the criterion that when the overall amino acid sequence identity was above 20%, they were denoted as homologues. Additionally, ORF 40 was determined to be homologous with SH1 ORF 52 because the ORFs shared a 210-bp region of 30% identity even though their overall identity remained below 20%. The identities between the corresponding translated ORFs ranged from 17.2 (HHIV-2 ORF 40 versus SH1 ORF 52) to 87.2% (HHIV-2 gene 14 versus SH1 gene 23), whereas in some genomic regions, there was no detectable similarity between ORFs (Fig. 4A and B; see Table S3 in the supplemental material). SH1 encodes six putative proteins containing predicted transmembrane helices (14). Five of them, excluding the ORF 15 product, have a homologue in the HHIV-2 genome.

The most conserved region between the genomes includes the genes coding for structural proteins (from HHIV-2 ORF 7 to gene 21) (Fig. 4D). The highest identities at the amino acid level were found in the putative ATPase (79.2%), major coat proteins VP4 and VP7 (82.3% and 72.4%, respectively), and major membrane protein VP12 (87.2%). In addition, the HHIV-2 genomic region spanning from ORF 30 to ORF 39 shares significant similarity to SH1 (Fig. 4A and B), especially ORFs 30, 31, and 36, which encode polypeptides (identities, 68.6 to 71.9%) (see Table S3 in the supplemental material). The remaining translated ORFs in this region show lower amino acid level identity (37.3 to 52.0%) to SH1 proteins, but most of them contain regions with an identity as high as 80%. Moreover, the largest structural protein, VP1 (194.5 kDa in HHIV-2 and 152.3 kDa in SH1), has a domain structure. The overall amino acid identity between VP1 proteins is only 21.3% (see Table S3). Nevertheless, the region of HHIV-2 VP1 residues 290 to 449, 481 to 585, and 1666 to 1775 have identities of 53,

43, and 65%, respectively, to the corresponding SH1 VP1 regions, suggesting that the proteins are related.

SH1 VP2 is a structural protein closely associated with the vertex complex (24). Sequence alignment showed that the first approximately 260 N-terminal amino acids of SH1 VP2 are absent in HHIV-2 VP2 (Fig. 4D). Although the overall amino acid identity between VP2 proteins is 26.1%, two separate domains in the VP2 polypeptide are rather highly conserved (identities, 63.3 and 56.1%) (Fig. 4D). Between the conserved domains, HHIV-2 VP2 contains a repeating stretch pattern previously reported for SH1 VP2 (heptapeptide repeat DXAARGY, where X is D/E and Y is A/S/T) (14). The amino acid identity of VP2 repeat domains between the viruses is low (25.6%). The HHIV-2 VP2 repeat sequence could be classified as a heptapeptide repeat, although not as clearly as the corresponding repeat sequence in SH1 VP2 (see Fig. S3 in the supplemental material). The main resemblance between these repeat sequences is that the first amino acid is acidic, either aspartic acid or glutamic acid.

There is a cluster of five ORFs/genes (ORFs 22 to 26) in HHIV-2 which are unique and have no homologues in the sequence databases. Two of them (genes 24 and 25) encode the HHIV-2 structural proteins VP16 and VP17. In SH1, the corresponding region (genes 31 to 33) codes for at least three SH1-specific structural proteins (VP3, VP6, and VP9), of which VP3 and VP6 form the spike structures at the 5-fold vertices. The spikes are known to be responsible for host recognition (24). Thus, VP16 and VP17 are potential candidates for forming the HHIV-2 spike complex. Other differences between these two haloviruses can be found in individual ORFs that are unique to each genome (Fig. 4A and B). The updated annotation of SH1 (44) suggests that SH1 may not have as many ORFs as described previously (14). The SH1 ORFs 1, 2, 3, and 56 located in the ITR regions are probably not transcribed, and they have no matches in the HHIV-2 genome (Fig. 4A and B).

DISCUSSION

The origin and evolution of viruses are often difficult to interpret, and there have been speculations on various different scenarios (20, 31). A fairly new approach considering the capsid organization and MCP structure to be the landmarks of viruses has let us approach viral evolution from an architectural point of view (1, 3, 10, 11, 16). Although nucleotide sequences are evolving rapidly and viral genes and genomes are extremely diverse, the protein structures are more conserved. The limited number of known virus structures remains a hindrance, especially among archaeal viruses. Thus, there is an inherent value in learning more about viruses to evaluate this hypothesis more profoundly. The first virus infecting archaea was isolated in 1974 from a hypersaline environment by Torsvik and Dundas (56). By the year 2011, approximately 100 archaeal viruses had been isolated and characterized (7, 42), which is a miniscule number compared to thousands of described bacterial viruses.

As for many other archaeal viruses described thus far, analyses of the genomes and genes are of limited value due to the lack of similarity to other sequences deposited in databases. Here, our comparison of the two related viruses allowed us to interpret the gene function and genome organization more thoroughly. HHIV-2 and SH1 have a similar genome synteny and size, demonstrating a close evolutionary relationship between the viruses (Fig. 4). However, the genetic similarity is unevenly distributed, not only throughout the genomes but also within single genes (Fig. 4). The other SH1-related genetic elements, *Haloarcula* plasmid pHH205, and integrated proviruses in the genomes of *Haloarcula* and *Halobacterium*, have only a few genes in common with SH1, whereas they are more similar to each other, suggesting a more distant evolutionary relationship (27). However, comparison of HHIV-2 genes against databases led to the discovery of a provirus in the genome of *H. paucihalophilus.* Nevertheless, it is unknown whether these genetic elements are still active viruses or only defective remnants of viruses.

Both *H. hispanica* icosahedral viruses have complex structures composed of several structural protein species (Fig. 3) (14). It is expected that HHIV-2 has a virion architecture similar to that of SH1, given that their virions have equal diameters (approximately 80 nm) (7, 24), their MCPs (VP4 and VP7) and major membrane proteins (VP10 and VP12) are homologous, and the entire virion protein patterns share common signatures (Fig. 3 and 4D). Our previous study (7) together with these data (Fig. 2A and D) suggest that there is a membrane under the HHIV-2 protein capsid. SH1, also an inner membrane-containing virus, has an unusual T=28 capsid architecture (24). The SH1 capsomers consist of two different MCPs together forming a hexagonal plane topped by tower structures (24). The homologous HHIV-2 and SH1 MCPs have seemingly similar copy numbers, and their molecular masses are almost identical, proposing similar tertiary MCP structures. The structural descriptions of archaeal SH1 and bacterial P23-77 virions have shown evolutionary connections that cannot be revealed by comparisons of nucleotide or amino acid sequence data (24, 25).

The sequence analyses and comparison of these two virus isolates demonstrate that the viral proteins can be dissected into a slowly evolving group responsible for conserved capsid architectures and a more rapidly changing group involved in interactions with the host, as has been previously suggested (11, 35). The SH1 spike complex proteins VP3 and VP6 and the nonhomologous HHIV-2 proteins VP16 and VP17 are encoded by genes that are located in similar positions in their genomes, clearly illustrating recent recombination events (Fig. 4). Both SH1 and HHIV-2 contain the large structural proteins VP1 and VP2. In SH1, VP2 has been shown to be associated with the VP3-VP6 vertex complex (24, 29). Comparison of SH1 and HHIV-2 VP1 and VP2 sequences suggests that some parts of the corresponding genes have evolved more rapidly than others (Fig. 4D). It is likely that the conserved areas are involved in encoding the homologous capsid structures. The less conserved areas might be those associated with the more rapidly evolved spike proteins. Given the vertex position for VP2 (24), it might function in stabilizing the connection among the capsid, spike complex, and the underlying membrane. Despite SH1 and HHIV-2 having different genes for putative spike structures and the adsorption rates of the viruses varying substantially (Fig. 1E), the host ranges of the viruses are the same, including two *Haloarcula* strains. The receptor molecules for both viruses remain unknown. To avoid host resistance to infection, the host-recognizing structures of viruses are prone to variation. This has been shown among very closely related viruses (50) and also for the crenarchaeal *Sulfolobus* turreted icosahedral viruses STIV and STIV-2, which share capsid organization similarity to PRD1 but have strikingly different vertex structures (23, 46).

Isolating and studying more structures of icosahedral viruses from the domain *Archaea* are crucial to gaining understanding of not only viruses but also the ancient division of the three domains

of life. It is also of importance to demonstrate that archaeal viruses are an essential part of the virosphere, with their evolutionary origin being shared with other viruses. Resolving a detailed structure of the HHIV-2 capsid and its proteins is the next step to be taken.

ACKNOWLEDGMENTS

This work was supported by the Academy of Finland Centre of Excellence Program in Virus Research grant 11296841 (2006 to 2011 to J.K.H.B. and D.H.B), Academy Professor (Academy of Finland) funding grants 255342 and 256518 (D.H.B.), Academy of Finland grants (127665 to H.M.O. and 251013 to M.J.), and Maj and Tor Nessling Foundation grants (2010098 and 2011162 to J.K.H.B.). S.T.J. is a fellow of the Viikki Doctoral Programme in Molecular Biosciences, and R.K.P. is a member of the Biological Interactions Graduate School. We thank the University of Helsinki for the support to EU ESFRI Instruct Associate Centre for Virus Production and Purification used in this study.

We thank Nisse Kalkkinen for a long-standing collaboration in protein chemistry. We acknowledge Nina Atanasova, Ausra Domanska, Nadine Fornelos Martins, Sari Korhonen, Elina Laanto, Sigita Pangonyte, Petri Papponen, and Soile Storman for their skillful technical assistance.

REFERENCES

1. **Abrescia NGA, Bamford DH, Grimes JM, Stuart DI.** Structure unifies the viral universe. Annu. Rev. Biochem., in press.
2. **Abrescia NGA, et al.** 2008. Insights into virus evolution and membrane biogenesis from the structure of the marine lipid-containing bacteriophage PM2. Mol. Cell **31**:749–761.
3. **Abrescia NGA, Grimes JM, Ravantti JJ, Bamford DH, Stuart DI.** 2010. What does it take to make a virus: the concept of the viral "self," p 35–58. *In* Stockley PG, Twarock R (ed), Emerging topics in physical virology. Imperial College Press, London, United Kingdom.
4. **Adams MH.** 1959. Bacteriophages. Interscience Publishers, Inc., New York, NY.
5. **Altschul SF, et al.** 1997. Gapped BLAST and PSI-BLAST: a new generation of protein database search programs. Nucleic Acids Res. **25**:3389–3402.
6. **Anderson I, et al.** 2011. Novel insights into the diversity of catabolic metabolism from ten haloarchaeal genomes. PLoS One **6**:e20237.
7. **Atanasova NS, Roine E, Oren A, Bamford DH, Oksanen HM.** 2012. Global network of specific virus-host interactions in hypersaline environments. Environ. Microbiol. **14**:426–440.
8. **Bahar MW, Graham SC, Stuart DI, Grimes JM.** 2011. Insights into the evolution of a complex virus from the crystal structure of vaccinia virus D13. Structure **19**:1011–1020.
9. **Baliga NS, et al.** 2004. Genome sequence of *Haloarcula marismortui*: a halophilic archaeon from the Dead Sea. Genome Res. **14**:2221–2234.
10. **Bamford DH.** 2003. Do viruses form lineages across different domains of life? Res. Microbiol. **154**:231–236.
11. **Bamford DH, Grimes JM, Stuart DI.** 2005. What does structure tell us about virus evolution? Curr. Opin. Struct. Biol. **15**:655–663.
12. **Bamford DH, Mindich L.** 1984. Characterization of the DNA-protein complex at the termini of the bacteriophage PRD1 genome. J. Virol. **50**: 309–315.
13. **Bamford DH, Mindich L.** 1980. Electron microscopy of cells infected with nonsense mutants of bacteriophage φ6. Virology **107**:222–228.
14. **Bamford DH, et al.** 2005. Constituents of SH1, a novel lipid-containing virus infecting the halophilic euryarchaeon *Haloarcula hispanica.* J. Virol. **79**:9097–9107.
15. **Bartolomé B, Jubete Y, Martínez E, de la Cruz F.** 1991. Construction and properties of a family of pACYC184-derived cloning vectors compatible with pBR322 and its derivatives. Gene **102**:75–78.
16. **Benson SD, Bamford JK, Bamford DH, Burnett RM.** 1999. Viral evolution revealed by bacteriophage PRD1 and human adenovirus coat protein structures. Cell **98**:825–833.
17. **Bergh O, Borsheim KY, Bratbak G, Heldal M.** 1989. High abundance of viruses found in aquatic environments. Nature **340**:467–468.
18. **Bradford MM.** 1976. A rapid and sensitive method for the quantitation of microgram quantities of protein utilizing the principle of protein-dye binding. Anal. Biochem. **72**:248–254.
19. **Dyall-Smith M (ed).** The halohandbook: protocols for halobacterial genetics. M. Dyall-Smith, Martinsried, Germany. http://www.haloarchaea.com/resources/halohandbook/Halohandbook_2009_v7.1.pdf.
20. **Forterre P.** 2006. The origin of viruses and their possible roles in major evolutionary transitions. Virus Res. **117**:5–16.
21. **Gorbalenya AE, Koonin EV.** 1989. Viral proteins containing the purine NTP-binding sequence pattern. Nucleic Acids Res. **17**:8413–8440.
22. **Guixa-Boixareu N, Calderón-Paz J, Heldal M, Bratbak G, Pedrós-Alió C.** 1996. Viral lysis and bacterivory as prokaryotic loss factors along a salinity gradient. Aquat. Microb. Ecol. **11**:215–227.
23. **Happonen LJ, et al.** 2010. Familial relationships in hyperthermo- and acidophilic archaeal viruses. J. Virol. **84**:4747–4754.
24. **Jäälinoja HT, et al.** 2008. Structure and host-cell interaction of SH1, a membrane-containing, halophilic euryarchaeal virus. Proc. Natl. Acad. Sci. U. S. A. **105**:8008–8013.
25. **Jaatinen ST, Happonen LJ, Laurinmäki P, Butcher SJ, Bamford DH.** 2008. Biochemical and structural characterisation of membrane-containing icosahedral dsDNA bacteriophages infecting thermophilic *Thermus thermophilus.* Virology **379**:10–19.
26. **Jalasvuori M, et al.** 2009. The closest relatives of icosahedral viruses of thermophilic bacteria are among viruses and plasmids of the halophilic archaea. J. Virol. **83**:9388–9397.
27. **Jalasvuori M, Pawlowski A, Bamford JKH.** 2010. A unique group of virus-related genome integrating elements found solely in the bacterial family *Thermaceae* and the archaeal family *Halobacteriaceae.* J. Bacteriol. **192**:3231–3234.
28. **Juez G, Rodriquez-Valera F, Ventosa A, Kushner DJ.** 1986. *Haloarcula hispanica* spec. nov. and *Haloferax gibbonsii* spec. nov., two new species of extremely halophilic archaebacteria. Syst. Appl. Microbiol. **8**:75–79.
29. **Kivelä HM, et al.** 2006. Quantitative dissociation of archaeal virus SH1 reveals distinct capsid proteins and a lipid core. Virology **356**:4–11.
30. **Klein R, et al.** 2002. *Natrialba magadii* virus ΦCh1: first complete nucleotide sequence and functional organization of a virus infecting a haloalkaliphilic archaeon. Mol. Microbiol. **45**:851–863.
31. **Koonin EV, Dolja VV.** 2006. Evolution of complexity in the viral world: the dawn of a new vision. Virus Res. **117**:1–4.
32. **Koonin EV, Senkevich TG, Chernos VI.** 1993. Gene A32 product of vaccinia virus may be an ATPase involved in viral DNA packaging as indicated by sequence comparisons with other putative viral ATPases. Virus Genes **7**:89–94.
33. **Krogh A, Larsson B, von Heijne G, Sonnhammer EL.** 2001. Predicting transmembrane protein topology with a hidden Markov model: application to complete genomes. J. Mol. Biol. **305**:567–580.
34. **Krupovič M, Bamford DH.** 2010. Order to the viral universe. J. Virol. **84**:12476–12479.
35. **Krupovič M, Bamford DH.** 2008. Virus evolution: how far does the double beta-barrel viral lineage extend? Nat. Rev. Microbiol. **6**:941–948.
36. **Laurinavičius S, Käkelä R, Somerharju P, Bamford DH.** 2004. Phospholipid molecular species profiles of tectiviruses infecting Gram-negative and Gram-positive hosts. Virology **322**:328–336.
37. **Matsushita I, Yanase H.** 2009. The genomic structure of *Thermus* bacteriophage ΦIN93. J. Biochem. **146**:775–785.
38. **Nandhagopal N, et al.** 2002. The structure and evolution of the major capsid protein of a large, lipid-containing DNA virus. Proc. Natl. Acad. Sci. U. S. A. **99**:14758–14763.
39. **Ng WV, et al.** 2000. Genome sequence of *Halobacterium* species NRC-1. Proc. Natl. Acad. Sci. U. S. A. **97**:12176–12181.
40. **Nuttall SD, Dyall-Smith ML.** 1993. Ch2, a novel halophilic archaeon from an Australian solar saltern. Int. J. Syst. Bacteriol. **43**:729–734.
41. **Oren A.** 2002. Diversity of halophilic microorganisms: environments, phylogeny, physiology, and applications. J. Ind. Microbiol. Biotechnol. **28**:56–63.
42. **Pina M, Bize A, Forterre P, Prangishvili D.** 2011. The archeoviruses. FEMS Microbiol. Rev. **35**:1035–1054.
43. **Porter K, et al.** 2005. SH1: A novel, spherical halovirus isolated from an Australian hypersaline lake. Virology **335**:22–33.
44. **Porter K, Russ BE, Yang J, Dyall-Smith ML.** 2008. The transcription programme of the protein-primed halovirus SH1. Microbiology **154**: 3599–3608.
45. **Ravantti JJ, Gaidelyte A, Bamford DH, Bamford JK.** 2003. Comparative analysis of bacterial viruses Bam35, infecting a gram-positive host, and PRD1, infecting gram-negative hosts, demonstrates a viral lineage. Virology **313**:401–414.

46. **Rice G, et al.** 2004. The structure of a thermophilic archaeal virus shows a double-stranded DNA viral capsid type that spans all domains of life. Proc. Natl. Acad. Sci. U. S. A. **101**:7716–7720.
47. **Rohrmann GF, Cheney R, Pauling C.** 1983. Bacteriophages of *Halobacterium halobium*: virion DNAs and proteins. Can. J. Microbiol. **29**:627–629.
48. **Roine E, Oksanen HM.** 2011. Viruses from the hypersaline environment, p 153–172. *In* Ventosa A, Oren A, Ma Y (ed), Halophiles and hypersaline environments: current research and future trends. Springer-Verlag, Berlin, Germany.
49. **Rux JJ, Kuser PR, Burnett RM.** 2003. Structural and phylogenetic analysis of adenovirus hexons by use of high-resolution X-ray crystallographic, molecular modeling, and sequence-based methods. J. Virol. **77**:9553–9566.
50. **Saren A-M, et al.** 2005. A snapshot of viral evolution from genome analysis of the *Tectiviridae* family. J. Mol. Biol. **350**:427–440.
51. **Schägger H, von Jagow G.** 1987. Tricine-sodium dodecyl sulfate-polyacrylamide gel electrophoresis for the separation of proteins in the range from 1 to 100 kDa. Anal. Biochem. **166**:368–379.
52. **Sime-Ngando T, et al.** 2011. Diversity of virus-host systems in hypersaline Lake Retba, Senegal. Environ. Microbiol. **13**:1956–1972.
53. **Srinivasiah S, et al.** 2008. Phages across the biosphere: contrasts of viruses in soil and aquatic environments. Res. Microbiol. **159**:349–357.
54. **Strömsten NJ, Bamford DH, Bamford JKH.** 2005. In vitro DNA packaging of PRD1: a common mechanism for internal-membrane viruses. J. Mol. Biol. **348**:617–629.
55. **Suttle CA.** 2007. Marine viruses—major players in the global ecosystem. Nat. Rev. Microbiol. **5**:801–812.
56. **Torsvik T, Dundas ID.** 1974. Bacteriophage of *Halobacterium salinarium*. Nature **248**:680–681.
57. **Walker JE, Saraste M, Runswick MJ, Gay NJ.** 1982. Distantly related sequences in the alpha- and beta-subunits of ATP synthase, myosin, kinases and other ATP-requiring enzymes and a common nucleotide binding fold. EMBO J. **1**:945–951.
58. **Ye X, Ou J, Ni L, Shi W, Shen P.** 2003. Characterization of a novel plasmid from extremely halophilic Archaea: nucleotide sequence and function analysis. FEMS Microbiol. Lett. **221**:53–57.

JVI Journals.ASM.org

ERRATUM

Closely Related Archaeal *Haloarcula hispanica* Icosahedral Viruses HHIV-2 and SH1 Have Nonhomologous Genes Encoding Host Recognition Functions

Salla T. Jaakkola, Reetta K. Penttinen, Silja T. Vilén, Matti Jalasvuori, Gunilla Rönnholm, Jaana K. H. Bamford, Dennis H. Bamford, and Hanna M. Oksanen

Institute of Biotechnology and Department of Biosciences, University of Helsinki, Helsinki, Finland; Department of Biological and Environmental Science and Nanoscience Center, Jyväskylä, Finland; and Institute of Biotechnology, University of Helsinki, Helsinki, Finland

Volume 86, no. 9, p. 4734–4742, 2012. Page 4741, Acknowledgments, paragraph 1: The first sentence should read: "This work was supported by the Academy of Finland Centre of Excellence Program in Virus Research grant 11296841 (2006 to 2011 to J.K.H.B. and D.H.B.), Academy Professor (Academy of Finland) funding grants 256197 and 256518 (D.H.B.), Academy of Finland grants (127665 to H.M.O. and 251013 to M.J.), and Maj and Tor Nessling Foundation grants (2010098 and 2011162 to J.K.H.B.)."

doi:10.1128/JVI.00860-12